

Acoustic scintillations and angle-of-arrival fluctuations observed outdoors with a large planar vertical microphone array

D. Keith Wilson and Calandra R. Tate

*Information Science and Technology Directorate, U.S. Army Research Laboratory,
Adelphi, Maryland 20783*

dkwilson@arl.mil

David C. Swanson and Karl M. Reichard

*Applied Research Laboratory, Pennsylvania State University,
State College, Pennsylvania 16804*

Abstract: A vertical planar array of 32 microphones (eight elements in the vertical direction and four in the horizontal; overall dimensions approximately 6 m by 3 m) was used to image the scintillations and angle-of-arrival fluctuations from a source 770 m distant. Data sets of 20-min duration were collected in a variety atmospheric conditions. On a windy afternoon, the source image underwent dramatic scintillations and fluctuations in its apparent position. For still nighttime conditions, the image was much more stable, although deep fading still occurred.

©1999 Acoustical Society of America

PACS numbers: 43.28.Fp, 43.60.Gk

1. Introduction

Arrays of microphones can be used to track acoustic sources moving through the atmosphere [Ferguson and Criswick, 1996; Pham and Sadler, 1996]. The atmosphere is hardly a passive participant in the process: random fluctuations in the wind and temperature fields drive random variations in the intensity and orientation of acoustic wave fronts impinging on the array. Although analogous problems have been studied in other areas of wave propagation (see, for example, the discussion in Flatte *et al.* [1979] regarding ocean acoustics), there have been few systematic observations of wave front angle-of-arrival variability for acoustic propagation in the atmosphere. Earlier related experiments have characterized sound-field statistics such as phase and amplitude structure functions [Bass *et al.*, 1991] and spatial coherence [Havelock *et al.*, 1995]. In this study we observe angle-of-arrival variability for near-ground propagation using a 32-element, planar vertical microphone array. Images of the acoustic beamformer output during 20-min trials conducted in three distinct meteorological conditions are presented in MPEG format.

2. Description of the experiment

In June 1998 we assembled a planar vertical array of 32 microphones at Rock Springs, Pennsylvania, on agricultural land maintained by the Pennsylvania State University Agronomy Research Center. The microphones in the array were arranged in eight horizontal rows and four vertical columns. The spacing between the rows was 0.75 m, and the spacing between columns was 0.98 m. The array was supported with four vertical fiberglass beams, which were anchored in cement. The structure is shown in Fig. 1.



Fig. 1. Left: Fiberglass beams and anchors used to support the microphone array. Right: Close-up view of a microphone and the mounting bracket. Readers of the print version should refer to the color version of these pictures in the online archival version.

The on-axis beam pattern of the array at 250 Hz is shown in Fig. 2. The initial nulls occur at $\theta \simeq \pm 13^\circ$ and $\phi \simeq \pm 20^\circ$, where θ is the elevation angle, and ϕ the azimuthal angle. The initial sidelobes are at $\theta \simeq \pm 19^\circ$ and $\phi \simeq \pm 31^\circ$, with the corresponding levels being -13 and -12 dB.

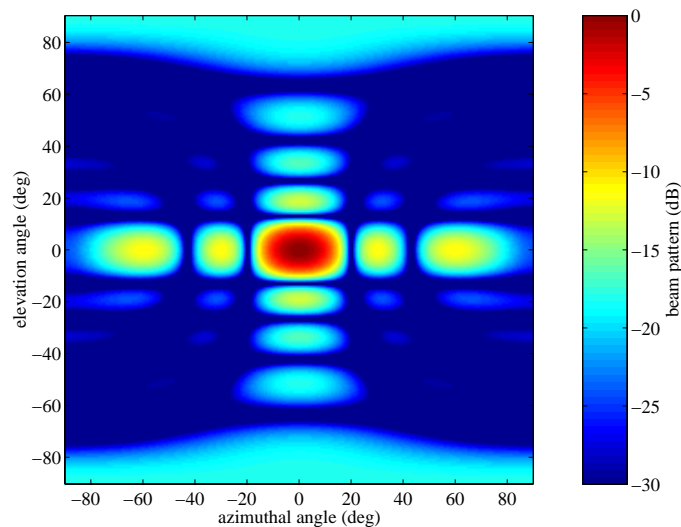


Fig. 2. Beam pattern of the array at $f = 240$ Hz, as a function of the azimuthal and elevation angles (both defined relative to normal incidence). Readers of the print version should refer to the color version of this figure in the online archival version.

The acoustic source in our experiment consisted of a pair of 18-in. woofers, each driven by a 200-W amplifier. The speakers were pointed toward each other and separated by 10 in., with the axis of the speakers perpendicular to the propagation path. By driving the speakers with opposite phases, a monopole-like radiation pattern in the far field was produced. Tones at 50, 100, 150, 200, and 250 Hz were broadcast. The height of the source above the ground was 1.2 m, and the distance from the microphone array was 770 m.

The signals from each of the 32 microphones were digitally sampled at 8000 Hz, thereby generating about 0.5 megabytes of data per second and a total of 585 megabytes per 20-min trial. The analog-to-digital conversion was accomplished using a dedicated PC board, model ADC64 by Innovative Integration. The data were transferred in real time to a PC hard disk. Upon completion of each trial, the data were saved to a recordable CD.

A total of six 20-min trials were run, encompassing several distinct meteorological conditions. The trials are summarized in Table 1. Three of these trials were selected for analysis here: 1738 and 2220 on 18 June, and 1033 on 19 June. The first of these trials took place on a moderately windy evening. Propagation was marginally downwind. The second trial was on a clear, still night, with a strong temperature inversion. The third was on a cloudy morning with light winds, shortly after a rain shower. The temperature gradient was very small for this final trial; in meteorological terminology such conditions are called *nearly neutral*.

Table 1. Summary of the six experimental trials. Time of day is in local daylight savings time. Direction is the angle between the propagation path and the wind vector (0° is downwind propagation, 180° is upwind). Temperature difference is the temperature at 2 m height minus the temperature at 10 m.

Date	Time of Day	Wind Speed (m/s)	Wind Dir. (deg off Array Axis)	Temperature Diff. ($^\circ\text{C}$)
18 June 1998	1536–1556	4.4	51	0.13
18 June 1998	1738–1758	2.3	61	–0.05
18 June 1998	2116–2136	0.3	149	–1.28
18 June 1998	2220–2240	0.1	169	–1.17
19 June 1998	0817–0837	0.8	116	–0.03
19 June 1998	1033–1053	0.4	160	0.10

3. Signal processing

Intensity and angle-of-arrival variability can be visualized by generating sequences of the beamformed array signals. By adjusting the phase of the signals prior to combining them, the main response axis of the array can be steered in different azimuthal and elevational directions. Scanning the main response axis over a large number of azimuthal and elevational directions yields a planar image of the energy arriving at the array. The process of combining the signals with various phase delays (beamforming) can be accomplished efficiently using a two-dimensional fast Fourier transform (2-D FFT). In this study we have chosen to use the 250-Hz component of the signal for imaging, because the ratio of array aperture to wavelength is most favorable for this frequency. Our signal processing method for constructing the images, which is based on common signal-processing techniques, is the following:

1. Load concurrent 80,000-point time series (10 s of data) for each of the microphones.
2. Partition each 80,000-point series into 10 segments. Apply a Hann window to the 8000-point segments and transform (1-D complex FFT) them to the frequency domain.
3. Select the 250 Hz frequency component from each FFT, thereby creating 8×4 complex matrices (representing the magnitude and phase at each microphone) for each of the 10 segments.
4. Average the 10 matrices to obtain a single 8×4 matrix representative of the 10-s interval.
5. Zero-pad the 8×4 matrix to 128×64 points and take the 2-D inverse FFT to create the image.
6. Repeat the process until the end of each 20-min time series is reached. The result is a total of 120 2-D images for each 20-min record.

Given the 8000-Hz sampling rate, the binwidth of each 8000-point FFT is exactly 1 Hz. Therefore the 250 Hz tone (like other integer frequencies) falls in the center of a bin. In actuality there is some modulation in the received frequency caused by atmospheric scattering. By using a longer FFT, we determined this modulation to be less than 0.1 Hz; therefore it does not significantly affect our results.

The padding procedure in Step 5 interpolates the image to a finer angular resolution. Equivalently, it artificially extends the vertical aperture of the array to $128\Delta z = 96$ m, where $\Delta z = 0.75$ m is the vertical sensor spacing. Therefore the 2-D inverse FFT has a vertical wavenumber axis $k_z = [-64, -63, \dots, 63] \Delta k_z$, where the wavenumber resolution is $\Delta k_z = 2\pi/(96 \text{ m}) = 0.0654 \text{ m}^{-1}$. Similarly, the horizontal aperture is $64\Delta y = 62.7$ m, where $\Delta y = 0.98$ m, and the horizontal wavenumber axis is $k_y = [-32, -31, \dots, 31] \Delta k_y$, where $\Delta k_y = 0.102 \text{ m}^{-1}$. For small arrival angles, $k_z \simeq k_0\theta$ and $k_y \simeq k_0\phi$ (where $k_0 = 2\pi f/c_0$ is the free-space wavenumber, c_0 is the approximate sound speed, and f is the frequency). Therefore, at 250 Hz (with $c_0 = 335$ m/s), the reconstructed image has interpolated angular resolution $\Delta\theta = 0.799^\circ$ and $\Delta\phi = 1.25^\circ$.

4. Acoustic images

MPEG files containing the sequences of beamformer images are presented in Mm. 1–3. For the session recorded on a windy afternoon (Mm. 1, starting at 1738 on 18 June), the source image was found to undergo dramatic scintillations. The fluctuations in received power have a dynamic range of about 20 dB and occur rapidly relative to the 10-s interval between images. The scintillations are much slower for the data recorded during still nighttime conditions (Mm. 2, 2220 on 18 June); however, a deep fade of about 8 dB, lasting several minutes, was still observed. The data recorded during light winds (Mm. 3, 1033 on 19 June) exhibit somewhat slower fluctuations than the previous windy afternoon, with the wave fronts arriving nearly vertically at the array. (In the sequences for both 1738 and 2220 on 18 June, faint sidelobes from the beamformer are occasionally evident near the bottom of the image. Note that the axes in Mm. 1–3 are $\pm 10^\circ$ elevation and $\pm 15^\circ$ azimuth, as opposed to the entire hemisphere shown in Fig. 2.)

Mm. 1. Beamformer image sequence for the trial beginning at 1738 on 18 June (906 Kb).

Mm. 2. Beamformer image sequence for the trial beginning at 2220 on 18 June (483 Kb).

Mm. 3. Beamformer image sequence for the trial beginning at 1033 on 19 June (894 Kb).

The signal level and angle-of-arrival fluctuations can be quantified using the peak (maximum) intensity in the images. Figures 3–5 show time series of the peak intensity for each of the three datasets and the arrival angles corresponding to the peak. The curves are broken off for records where the estimated SNR falls below 10 dB. (SNR was estimated from the difference between the power spectrum at 250 Hz and the average of 249 and 251 Hz) The intensity for the windy afternoon case (Fig. 3) underwent fluctuations with standard deviation 5.1 dB, close to the value of 5.6 dB characteristic of a strongly scattered wave [Flatté *et al.*, 1979]. The fluctuations occurred very rapidly, on time scales comparable to the 1 min. interval between images. The standard deviations of the elevation and azimuthal angles were 1.2° and 1.4° , respectively. These angular deviations are equivalent to displacements of 17 m in the vertical position and 18 m in the horizontal position of the virtual source. The mean elevation angle of the image was 3.7° , corresponding to a virtual source height of 50 m. Because our actual source was not this high, most of the energy reaching the array was likely refracted or scattered from above. The

mean azimuthal offset of 2.4° was approximately the same for all trials and therefore was likely due to imperfect alignment between the array axis and source bearing.

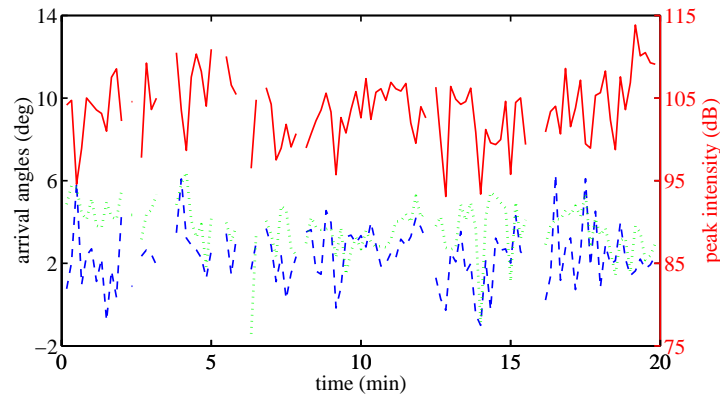


Fig. 3. Wave front angles of arrival and peak intensity at 250 Hz for the trial beginning at 1738 on 18 June 1998. Dotted line (green) is the elevation angle, dashed line (blue) is the azimuthal angle, and solid line (red) is the intensity.

The trial recorded during still nighttime conditions (Fig. 4) exhibited much more gradual changes in the intensity and angles of arrival. During the deep fade late in the trial, the elevation angle also decreased. Quite interestingly, a variation in the azimuthal angle was also observed during this event, indicating that the sound wave underwent significant refraction out of the vertical plane. The mean elevation angle was 6.1° (virtual source height of 83 m). Given the highly stable atmospheric conditions during this trial, clearly there must have been strong downward refraction of sound energy.

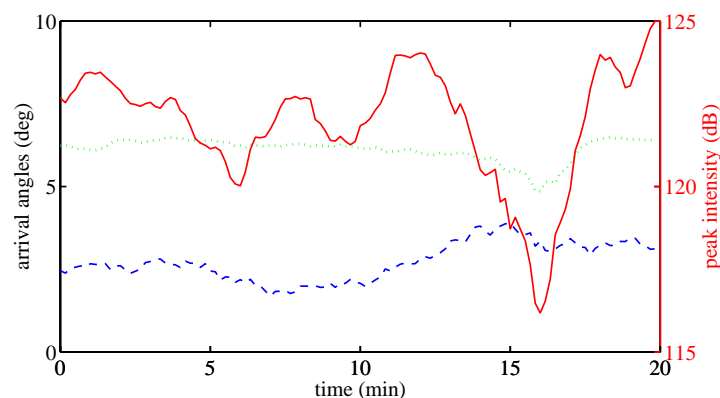


Fig. 4. Wave front angles of arrival and peak intensity for the trial beginning at 2220 on 18 June 1998. Legend is the same as Fig. 3.

The appearance of the trial recorded during light wind conditions (Fig. 5) is similar to the previous windy afternoon. The intensity fluctuations were only 1.6 dB, however, indicating that the wave was not strongly scattered. The standard deviations in the elevation and azimuthal angles were 0.47° and 0.56° , respectively. The center of the image was very close to the horizon (mean elevation angle 0.23°).

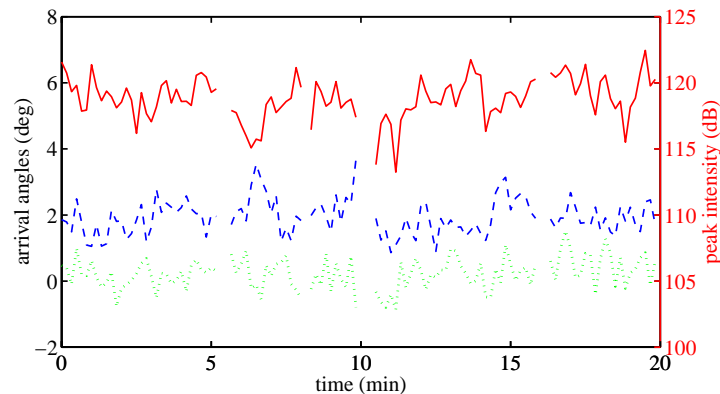


Fig. 5. Wave front angles of arrival and peak intensity for the trial beginning at 1033 on 19 June 1998. Legend is the same as Fig. 3.

5. Conclusion

The sequences of beamformer images in this study vividly demonstrate the dependence of acoustic scintillations and angle-of-arrival fluctuations on atmospheric conditions. On a windy afternoon, the fluctuations were rapid and characteristic of a strongly scattered wave. On a very still night, the image was much more stable, although an episode of deep fading lasting several minutes was still observed. Despite these differences, the windy afternoon and still night had in common that the source image was elevated several degrees above the horizon. On a cloudy morning with light winds, the image scintillated weakly and was positioned nearly on the horizon. The variability observed for the two daytime cases was driven by atmospheric turbulence of differing levels of intensity, whereas the nighttime variability likely resulted from gravity waves, which occur in temperature inversion layers of the atmosphere.

Acknowledgments

This work was funded through the U.S. Army Research Laboratory Director's Research Initiative Program. Jason Estep and Brian Magill (ARL/Penn State) helped build the array and assisted during execution of the experiment. Dr. Chenning Tong and Richard Thompson (Dept. of Meteorology/Penn State) maintained the atmospheric measurement systems.

References and links

- Bass, H. E., Bolen, L. N., Raspet, R., McBride, W., and Noble, J. (1991). "Acoustic propagation through a turbulent atmosphere: Experimental characterization," *J. Acoust. Soc. Am.* **90**, 3307–3313.
- Ferguson, B. G., and Criswick, L. G. (1996). "Variability in the bearing and range estimates of acoustic sources in air," *J. Acoust. Soc. Am.* **100**, 2636(A).
- Flatté, S. M., et al. (1979). *Sound Transmission Through a Fluctuating Ocean* (Cambridge University Press, Cambridge, England).
- Havelock, D. I., Di, X., Daigle, G. A., and Stinson, M. R. (1995). "Spatial coherence of a sound field in a refractive shadow: Comparison of simulation and experiment," *J. Acoust. Soc. Am.* **98**, 2289–2302.
- Pham, T., and Sadler, B. M. (1996). "Incoherent and coherent aeroacoustic wideband direction-finding algorithms for ground vehicles," *J. Acoust. Soc. Am.* **100**, 2636(A).